Degradation of HMG-CoA Reductase-induced Membranes in the Fission Yeast, *Schizosaccharomyces pombe*

Pek Yee Lum and Robin Wright

Department of Zoology, University of Washington, Seattle, Washington 98195

Abstract. Elevated levels of certain membrane proteins, including the sterol biosynthetic enzyme HMG-CoA reductase, induce proliferation of the endoplasmic reticulum. When the amounts of these proteins return to basal levels, the proliferated membranes are degraded, but the molecular details of this degradation remain unknown. We have examined the degradation of HMG-CoA reductase-induced membranes in the fission yeast, *Schizosaccharomyces pombe*. In this yeast, increased levels of the *Saccharomyces cerevisiae* HMG-CoA reductase isozyme encoded by *HMG1* induced several types of membranes, including karmellae, which formed a cap of stacked membranes that partially surrounded the nucleus. When expression of *HMG1* was repressed, the karmellae detached from the nucleus and formed concentric, multilayered membrane whorls that were then degraded. During the degradation process, CDCFDA-stained compartments distinct from preexisting vacuoles formed within the interior of the whorls. In addition to these compartments, particles that contained neutral lipids also formed within the whorl. As the thickness of the whorl decreased, the lipid particle became larger. When degradation was complete, only the lipid particle remained. Cycloheximide treatment did not prevent the formation of whorls. Thus, new protein synthesis was not needed for the initial stages of karmellae degradation. On the contrary, cycloheximide promoted the detachment of karmellae to form whorls, suggesting that a short lived protein may be involved in maintaining karmellae integrity. Taken together, these results demonstrate that karmellae membranes differentiated into self-degradative organelles. This process may be a common pathway by which ER membranes are turned over in cells.

CELLULAR membranes undergo dynamic changes in amount, composition, and morphology in response to changes in environmental or physiological conditions. Particularly striking and diverse are alterations of the endoplasmic reticulum that occur during cell development and differentiation. For example, as resting B cells differentiate into immunoglobulin-secreting plasma cells, the rough endoplasmic reticulum expands from a minor organelle into the most obvious structure in the cytoplasm (16, 56, 66, 72). In a similar way, smooth ER proliferation accompanies differentiation of steroid-hormone producing cells, including testis interstitial cells that synthesize androgens and lutein cells that synthesize progesterone (33). Alterations of ER organization are also observed in pathological situations, including infections by viruses, responses to drug treatments, and carcinogenesis (13, 27, 28, 43).

The balance between the synthesis and turnover of every cellular membrane is rigorously maintained throughout the life span of each cell. In certain cases, this balance is a critical feature of the cell's specialized function. For example, rod cells continuously shed discs from their apical surface, with the loss of membrane balanced by insertion of new discs at the base of the disc stack (37, 71). The balance between membrane synthesis and loss is dynamic: if the synthesis of new disc membranes is inhibited, such as by starvation for essential fatty acids, the rate of disc turnover is appropriately repressed (3). In spite of its important role in cellular function, a molecular description of how cells balance membrane assembly and degradation is not available for even a single membrane type.

Useful experimental models for analysis of membrane synthesis and turnover are provided by the specific membrane arrays induced by increased levels of certain ER membrane proteins (67). The best characterized of these membranes are formed in response to HMG-CoA reductase, the rate-limiting enzyme in sterol biosynthesis (4, 11, 42, 44, 55). In mammalian cells, increased amounts of HMG-CoA reductase lead to formation of crystalloid ER, which consist of hexagonally packed arrays of smooth ER tubules (4, 11). In budding yeast, increased levels of HMG-CoA reductase induce formation of karmellae, which are stacked membranes that partially surround the

Address all correspondence to Robin Wright, Dept. of Zoology, University of Washington, Seattle, WA 98195. Tel.: (206) 685-3651. Fax: (206) 543-3041.

nucleus (68). Crystalloid ER is maintained as long as HMG-CoA reductase levels are elevated. However, when HMG-CoA reductase levels are repressed by addition of LDL, the crystalloid ER is degraded (4, 42). Thus, the synthesis and degradation of a complex membrane structure can be simply and reproducibly controlled by experimentally altering the amount of HMG-CoA reductase.

One of our goals is to obtain a molecular description of karmellae biogenesis and degradation. However, the process of degradation has been difficult to study in budding yeast because, as in mammalian cells, degradation does not appear to involve easily distinguishable structural intermediates (4, 42; Koning, A. J., and R. Wright, unpublished results). This report describes karmellae degradation in the fission yeast, *Schizosaccharomyces pombe*. In contrast to karmellae in budding yeast, karmellae in *S. pombe* underwent a clear series of structural intermediates during degradation. This observation allowed us to analyze features of the degradation process. Our results indicated that karmellae degradation occurred by differentiation of detached karmellae into a self-degradative compartment. This process may offer opportunities to understand the molecular details of the turnover of endoplasmic reticulum membranes.

Materials and Methods

Yeast Strains, Media, and Growth Conditions

S. pombe strain ED665 (h^- leu1-32 ura4-D18 ade6-210) and SpB60 (h^+ leu1-32 ura4-D18 ade6-216) were obtained from P. Miller (University of Vermont, Burlington) and M. Moser (University of Washington, Seattle), respectively. Medium for growth of yeast cells was either YM-minus-Leucine (0.67% yeast nitrogen base without amino acids, 2% glucose, 0.1% yeast complete supplement minus leucine) or Edinburgh Minimal Medium (EMM) supplemented with 75 μg/ml adenine and 75 μg/ml uracil (40). EMM medium and yeast supplement minus leucine were purchased from Bio101 (La Jolla, CA). For solid medium, agar was added to 2% final concentration. Cells that expressed Hmg1p from the constitutive *adh+* promoter were grown in either YM-minus-Leucine or supplemented EMM. Cells that expressed Hmg1p from the repressible *nmt1+* promoter were grown in EMM supplemented with 75 μg/ml adenine and 75 μg/ml uracil (i.e., lack of thiamine) to induce *HMG1* expression and were grown in supplemented EMM with the addition of 6 μg/ml thiamine or in YM-minus-Leucine (which contains 0.4 μg/ml of thiamine).

Construction of Plasmids

Plasmids were constructed according to standard cloning procedures (5, 36). The vector, pART1, containing *Saccharomyces cerevisiae's LEU2* gene and the *S. pombe adh+* promoter was a gift from A. Klar (NCI-Frederick Cancer Research and Development Center, Frederick, MD) (39). The vector, pREP3X, with *S. cerevisiae's LEU2* gene and the *S. pombe nmt1+* promoter, was a gift from S. Forsburg (The Salk Institute, San Diego, CA) (21, 38). In pPL95, the *S. cerevisiae HMG1* gene was placed under the control of the constitutive *S. pombe adh+* promoter. To construct pPL95, a 4.0 kb BamH1/Nru1 restriction fragment from pJR435 (8), which contains the entire *HMG1* coding region and 3′ untranslated region, was made blunt by treatment with the Klenow fragment of DNA polymerase and ligated into the Sma1 site of pART1. In the plasmid pPL283, the *S. cerevisiae HMG1* gene was placed under the control of the repressible *S. pombe nmt1+* promoter, using an identical strategy as for pPL95.

Levels of Hmg1p Overexpression from nmt1 Promoter

The *nmt1+* promoter is strongly repressed by the presence of thiamine in the medium, but can induce as much as a 300-fold increase in gene expression in the absence of thiamine (39). Our attempts to estimate the level of overproduction of Hmg1p from the *nmt+* promoter were complicated by the absence of observable Hmg1p in thiamine-repressed cells. Without a baseline for the calculations, production of any observable Hmg1p would be an infinitely large overproduction. To estimate the minimal level of overproduction, we used NIH Image 1.54 Analysis software to compare the amount of Hmg1p on immunoblots produced at the peak of expression (24 h after induction) to the smallest observable amount of Hmg1p prepared from cells following repression (21 h after repression). Thus, we compared the highest amount of Hmg1p produced by the cells to the lowest observable amount. This approximation showed Hmg1p levels were increased at least 10- to 15-fold. Based on similar experiments, the level of overproduction of Hmg1p from the *adh+* promoter was comparable to that from the *nmt1+* promoter.

Staining of Cells and Microscopy

For $DiOC_6$ (3,3′-dihexyloxacarbocyanine iodide) staining (29), 2 μl of cell culture (OD_{600} = 0.5–1.0) were placed on a slide, mixed with 3 μl of an agar plus dye mixture, and covered with a coverslip. The agar plus dye mixture consisted of 200 μl of 1% SeaPlaque agarose (FMC Bioproducts, Rockland, ME) dissolved in medium and 1 μl of 10 mg/ml ethanolic $DiOC_6$ stock (Molecular Probes, Eugene, OR; Kodak, Rochester, NY). The dye/agar mixture was kept liquefied in a 50°C temperature block and used within 30 min of mixing. The quality of $DiOC_6$ staining depends on the physiology and the concentration of the cells (29). In the case of *S. pombe*, the nuclear envelope/ER in log phase cells stained well even with low concentrations of $DiOC_6$ (i.e., 30 μg/ml final concentration using the method described above). However, stationary phase cells required a higher concentration of dye to obtain nuclear membrane staining. In addition, log phase cells stained with $DiOC_6$ almost instantaneously, whereas stationary phase cells required a longer incubation time. Therefore, the dye concentration in the dye–agar mixture or the incubation time before viewing was increased or decreased to accommodate the different staining properties of cells during different stages of growth.

Nile Red (9-diethylamino-5H-benzo(α)phenoxazine-5-one) and R6 (rhodamine B, hexyl ester chloride) (both from Molecular Probes) were dissolved as a 10 mg/ml ethanolic stocks and used in a similar way as $DiOC_6$. The staining properties of R6 are identical to that of $DiOC_6$ (61), except that the excitation and emission wavelengths for the two dyes are different. Nile Red stains neutral lipids, so that both lipid particles and cellular membranes are visible in cells stained with Nile Red (22, 23). However, the intensity and the color of staining is different for lipid particles and membranes (22). In *S. pombe* stationary phase cells, cellular membranes were faintly stained, but lipid particles were stained prominently. In log phase cells, membranes and lipid particles had about equal staining intensity when the excitation wavelength was 568 nm (appropriate for rhodamine) but the lipid particles fluoresced brighter than membranes when the excitation wavelength was 488 nm (appropriate for fluorescein), making it easy to visualize lipid compartments enclosed by a whorl. This observation was consistent with the Nile Red staining properties in mammalian cells (22). The confocal micrographs shown in this paper of Nile Red staining used 488 nm as the excitation wavelength.

For double staining with both CDCFDA (carboxydichlorofluorescein diacetate; Molecular Probes) and R6 (60) the cells were first pelleted by centrifugation and resuspended in 1 ml of low pH YE medium (0.5% yeast extract, pH 3.5 with HCl). CDCFDA was added to a final concentration of 5 μM and incubated at 30°C on a rotator for 15 to 20 min (2, 46). After the dye had been taken up into the vacuoles of the cell, 3 μl of agar plus dye mixture containing R6 was mixed with 2 μl of CDCFDA-stained cell suspension as described for $DiOC_6$ staining.

For staining with FM1-43 (*N*-(3-triethylammoniumpropyl)-4-(*p*-dibutylaminostyryl) pyridinium, dibromide), 5 μl of 2 mM methanolic stock (Molecular Probes) was added to 5 ml of growing cell culture at 30°C. For double staining with CDCFDA, the cells were grown for 20 min in the presence of FM1-43, pelleted, and resuspended in 1 ml of low pH YE medium with 5 μM CDCFDA and the cultures were incubated at 30°C on a rotator for 15 to 20 min. For double staining cells with $DiOC_6$ and FM1-43, cells were allowed to induce karmellae in the presence of FM1-43 so that FM1-43 was present during the entire period of karmellae formation and degradation. 2 μl of the FM1-43–stained cells were spotted onto a slide and 3 μl of $DiOC_6$ plus agar mixture was added. The structure and the staining properties of FM1-43 were similar to those of FM4-64 (64).

Stained cells were observed with either conventional fluorescence optics, using a Nikon Microphot-FXA epifluorescence microscope, or confocal microscopy, using a BioRad MRC600 laser scanning confocal microscope. $DiOC_6$ and CDCFDA stained cells were observed with fluorescein filters (excitation 480 ± 20 nm, barrier 535 ± 40 nm) and R6- and FM1-43–stained cells were observed with rhodamine filters (Nikon DM580 Filter

set, excitation 546 nm, barrier 590 nm) on an epifluorescence microscope. Nile Red stained cells were either observed with fluorescein filters or rhodamine filters on an epifluorescence microscope. For confocal microscopy of cells stained with $DiOC_6$, CDCFDA or Nile Red, 488-nm excitation wavelength and BHS emission filter were used. For confocal microscopy of cells stained with R6 or FM1-43, 568-nm excitation wavelength and YHS emission filter were used. For confocal microscopy of double-stained cells, K1 and K2 filter blocks (560 DRLP dichroic, 522 DF35 green emission filter and 585 EFLP red emission filter) were used with the dual excitation filter on the filter wheel of the MRC600 microscope.

Electron Microscopy

Cells expressing Hmg1p from the *adh+* promoter were grown to early logarithmic phase at 30°C in EMM supplemented with 75 μg/ml adenine and 75 μg/ml uracil. Preparation for electron microscopy was a variation on that described in (70). The cell culture (40 ml) was mixed with 10 ml of 5× fixative (5× TBS [0.5 M Trizma base, 0.05 M KCl, 2.7 M NaCl] containing 5 mM $CaCl_2$, 5 mM $MgCl_2$, 1 M sorbitol, and 10% glutaraldehyde) and allowed to fix for 5 min at room temperature. Cells were then pelleted by centrifugation at 2,000 rpm in a clinical centrifuge and resuspended in 12.5 ml of 1× fixative. After incubating at room temperature for 30 min, the cells were washed four times with 20 ml of distilled water. The cells were then resuspended in 2 ml of distilled water, 2 ml of 4% potassium permanganate was added, and the mixture was incubated at room temperature for 5 min. The cells were pelleted and the fixative was replaced with 6 ml of 2% potassium permanganate. The cells were then incubated at room temperature for 1 h. Cells were washed extensively in distilled water, until no trace of purple color was evident, and dehydrated through a graded ethanol series and embedded in Pelco Ultra Low Viscosity Resin (Ted Pella, Redding, CA). The resin was allowed to polymerize for 48 h at 60°C. Silver-to-gold sections (~90 nM thick) were cut using a diamond knife and mounted on 200-mesh nickel grids. Sections were stained with 2% aqueous uranyl acetate and Reynold's lead citrate (49). Observations were made on a Philips 300 microscope operated at 60 kV.

Polyacrylamide Gel Electrophoresis and Immunoblotting

A total membrane fraction was prepared from yeast cells using modifications of the method described by Deschenes and Broach (15). Briefly, cells were harvested by centrifugation and resuspended in lysis buffer (0.3 M sorbitol, 0.1 M NaCl, 5 mM $MgCl_2$, and 10 mM Tris-HCl, pH 7.4) containing 1 μg/ml each TPCK (*N*-tosyl-L-phenylalanine chloromethyl ketone), leupeptin, pepstatin A, and 1 mM PefaBloc SC (Boehringer Mannheim Corp. Indianapolis, IN) in a screw cap microcentrifuge tube. Acid-washed glass beads were added to the meniscus and the sample was agitated at 4°C in a Mini-Beadbeater (Baxter, Redmond, WA) in two 1-min bursts, with a short incubation on ice between agitations. To maximize recovery of lysate after beadbeating, a hole was made on the cap of the microcentrifuge tube with a needle and the tube was placed upside down in a 5-ml conical plastic tube. The lysate was removed from the beads by centrifugation at 2,000 rpm for 5 min, in a clinical centrifuge. This method allowed complete recovery of the lysate.

A soft pellet, designated P1, was obtained following centrifugation in the clinical centrifuge. The supernatant solution was removed and centrifuged at top speed in a microcentrifuge for 20 min to obtain pellet P2. Hmg1p was present in both P1 and P2, but absent from the final supernatant solution. Either P1 or P2 fractions alone, or P1 and P2 combined, reproducibly provided identical estimates of the relative Hmg1p levels in all strains and conditions used in this study. In the immunoblots shown in this paper, P1 was used. Pellets were resuspended in 5 μl of lysis buffer per 10^7 cells and 1/2 volume of 2× sample buffer (0.06 M Tris-HCl, pH 6.8, 4% SDS, 20% glycerol, 10% β-mercaptoethanol, 0.01% Bromphenol blue) was added (30). The sample was heated for 15 min at 60°C and then centrifuged in a microcentrifuge at top speed for 5 min to pellet insoluble material. The supernatant solution, containing solubilized proteins from cellular membranes, was divided into aliquots and stored at 76°C until use. The proteins in the samples were separated on 7.5% polyacrylamide minigels, using a 3% stacking gel. After electrophoresis, the proteins were transferred to two stacked pieces of nitrocellulose in the Trans-Blot SD Semi-Dry Electrophoretic Transfer Cell (Bio Rad Labs., Richmond, CA) at 12V for 30 min. After transfer, the piece of nitrocellulose touching the gel was used for immunoblotting and the second piece was stained for total protein in TBST buffer (1× TBS, 0.05% Tween-20) with Indian ink (25) to control for uniform transfer. After blocking in TBSTM (1× TBS, 0.05% Tween-20, 2% nonfat milk) for 30 min, the immunoblot was incubated for 1 h in 1:7,500 dilution of polyclonal anti-Hmg1p antiserum in TBSTM (68). Following four washes in TBSTM, the immunoblot was incubated for 1 h in alkaline phosphatase-conjugated goat anti-rabbit antiserum (Promega, Madison, WI) diluted 1:7,500 in TBSTM. The blot was then washed four times with TBSTM, followed by quick washes in 500 ml of TBST and 500 ml of TBS. The blot was developed using 10 μg/ml NBT (nitroblue tetrazolium) and 5 μg/ml BCIP (5-bromo-4-chloro-3-indoyl phosphate) in developing buffer (0.1 M Tris-HCl, pH 9.5, 0.1 M NaCl, 5 mM $MgCl_2$) (26). Dried gels and the Western blots were digitized using a Scan-X Color Scanner (HSD Microcomputer, Mountain View, CA). Relative amounts of total protein loaded per lane as well as relative amounts of Hmg1p protein on the Western blot were determined using the NIH Image 1.54 Analysis software. Dilutions of each sample were loaded and analyzed to make certain that bands on the immunoblots were in the linear range of the alkaline phosphate reaction.

Results

Expression of the S. cerevisiae HMG1 Gene in S. pombe Induced Membrane Proliferations, Including Karmellae and Cytoplasmic Whorls

Human or hamster HMG-CoA reductase induces karmellae in budding yeast, rather than crystalloid ER (69). Conversely, expression of the budding yeast *HMG1* gene in mammalian cells produces crystalloid ER formation (69). These results indicate that elevated HMG-CoA reductase levels from heterologous sources can initiate membrane synthesis, but the organization of the resulting membranes is determined by the cell type in which the proliferation occurs. To examine features of karmellae formation and degradation that were difficult to observe in *S. cerevisiae*, we tested whether or not these observations could be extended to fission yeast.

For these experiments, the *S. cerevisiae HMG1* gene was placed under the control of the *adh+* promoter, an *S. pombe* promoter that is expressed constitutively in glucose- or glycerol/ethanol-grown cells (21, 39, 52). To analyze membranes induced by Hmg1p, stationary phase cells containing pPL95, a multi-copy plasmid with the *adh+: HMG1* promoter fusion gene, were inoculated into fresh medium and allowed to resume growth and overproduce Hmg1p. Increased levels of HMG-CoA reductase activity confer resistance to competitive inhibitors, such as compactin and lovastatin (1, 19, 50). The Hmg1p produced by *S. pombe* was functional, since it enabled the cells to grow in the presence of 100 μg/ml lovastatin, which was lethal to wild-type *S. pombe* cells (data not shown).

The organization of subcellular membranes in cells expressing *HMG1* under control of the *adh+* promoter was observed using fluorescence microscopy of $DiOC_6$-stained cells and transmission electron microscopy. Several types of membrane arrays were induced by Hmg1p, including peripheral membrane stacks near the plasma membrane (referred to as "strips"), karmellae, and multilayered membrane whorls in the cytoplasm (Figs. 1 and 2). The karmellae that formed in *S. pombe* appeared identical to that observed in budding yeast (68). As in *S. cerevisiae*, the karmellae membranes were also asymmetrically arranged on the nucleus and were usually asymmetrically segregated at mitosis. The whorls were frequently found in close proximity to the nucleus or karmellae (Fig. 1, *3a* and *3b* and Fig. 2).

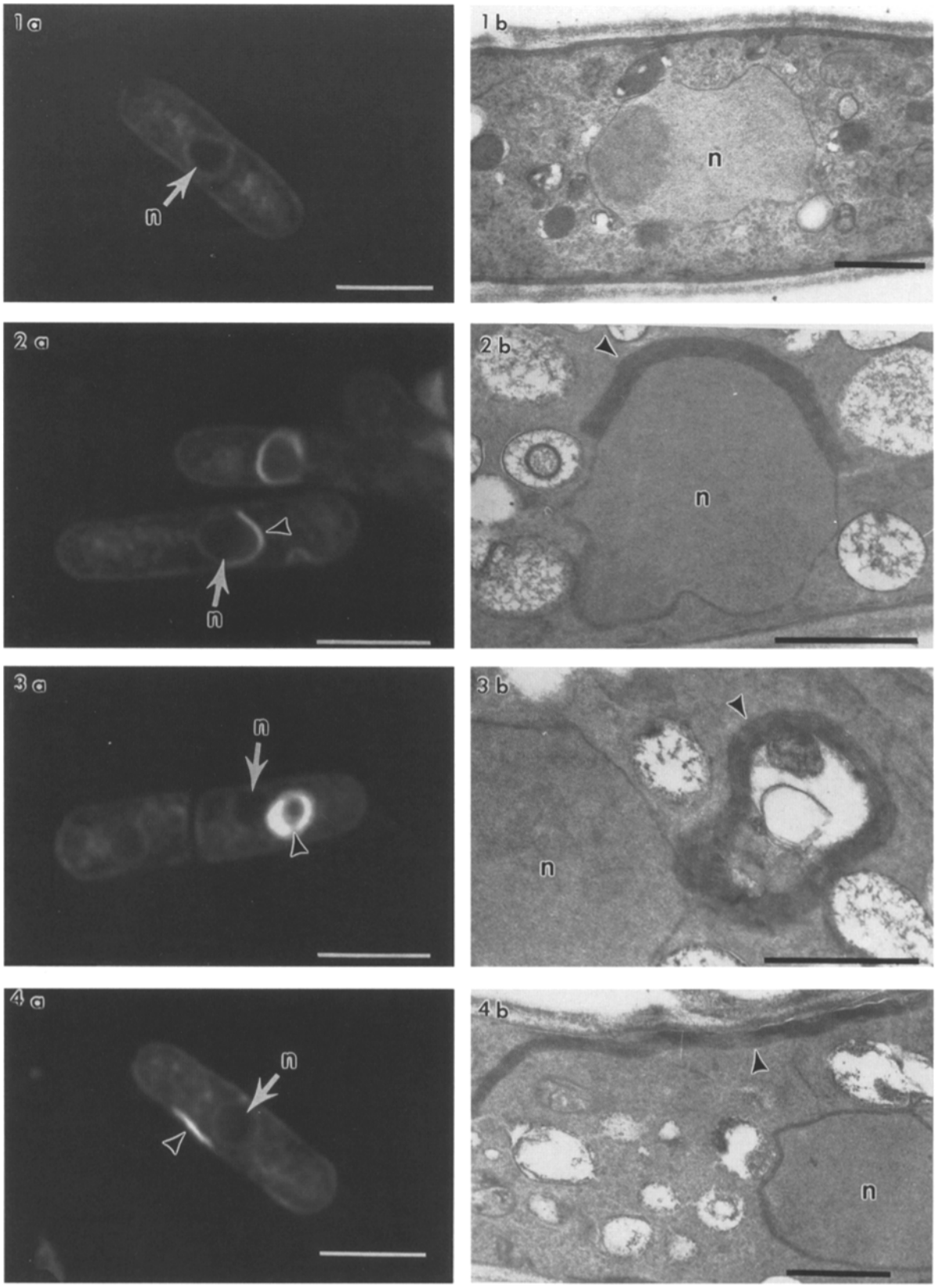

Figure 1. Expression of the *S. cerevisiae* Hmg1p in *S. pombe* induced several types of membrane arrays. The cells shown here contain pPL95, a multicopy plasmid with an *adh+:HMG1* promoter fusion. The left column (*a*) shows confocal micrographs of living cells stained with $DiOC_6$. The right column (*b*) shows electron micrographs of cells containing the same membrane type. (*1a* and *1b*) Cells that lack Hmg1p did not contain membrane proliferations. $DiOC_6$ stained the nuclear envelope and the ER in these cells. (*2a* and *2b*) Nuclear-associated membranes known as karmellae were produced in cells that expressed *HMG1*. (*3a* and *3b*) Whorls of stacked membranes were present in cells that expressed *HMG1*. Note that whorls were often found adjacent to the nucleus. (*4a* and *4b*) Strips of stacked membranes near the cell periphery were present in cells that expressed HMG1. *n*, nucleus. Arrowheads point to proliferated membranes. Bars: (*1a–4a*) 5 μm; (*1b–4b*) 1 μm.

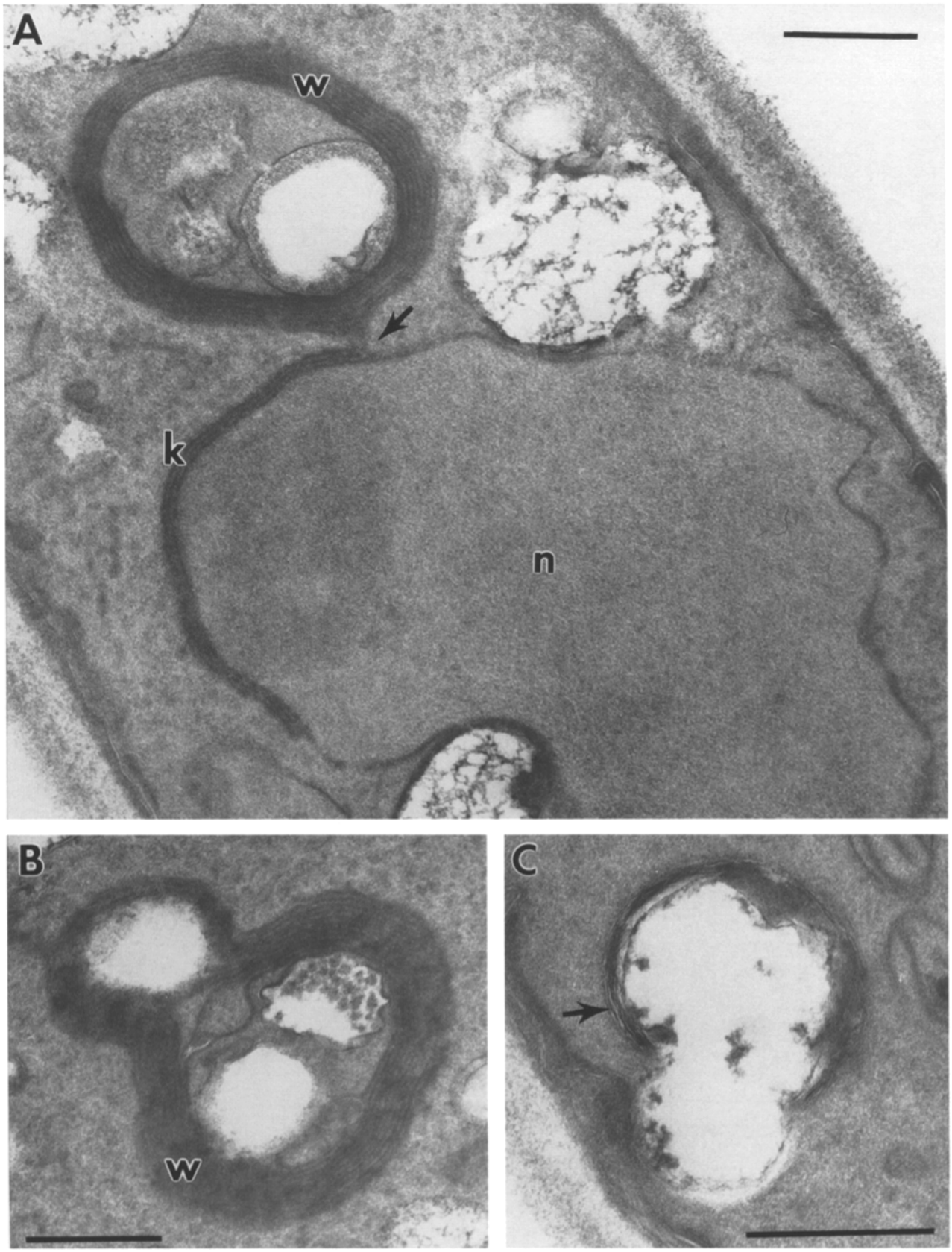

Figure 2. In cells with proliferated membranes, whorls of stacked membranes were frequently present near the nucleus. The cells in this panel are expressing *HMG1* under control of the *adh+* promoter. (*A*) Whorls were often present near the nucleus (see also Fig. 1, *3a* and *3b*, and Fig. 11 A). Arrow shows a possible connection between karmellae and a whorl. (*B*) Several compartments were present in the whorl interior. Based on fluorescence staining properties described later, two types of compartments were present within the whorl: CDCFDA-stained compartments and lipid particles. (*C*) As degradation progressed, the number of whorl layers decreased and the layers became less organized. *n*, nucleus; *w*, whorl; *k*, karmellae. Bars, 0.5 μm.

These observations were consistent with previous conclusions that membrane biogenesis can be induced by HMG-CoA reductase molecules from heterologous sources (69). In addition, they provided the opportunity to examine the relationships among clearly distinguishable membrane types, particularly karmellae and whorls.

The Types of Membrane Proliferations Produced Depended on the Growth Phase of the Culture

The expression pattern of *HMG1* under the control of the *adh+* promoter resulted in increased levels of Hmg1p during logarithmic growth and in decreasing levels of Hmg1p as the cells entered stationary phase (data not shown). Thus, the expression pattern of the *adh+* promoter provided a way to determine whether karmellae and whorls were temporally related. We examined the changes in membrane morphology of cells with the *adh+:HMG1* promoter fusion (pPL95) throughout culture growth (Fig. 3). During lag phase growth, peripheral membrane stacks (strips) were the predominant membrane type, present in ~40% of the cells in the population. The peak of membrane induction occurred in mid-log phase growth, when more than 80% of the cell population contained proliferated membranes. Proliferated membranes were never observed in all cells, at least in part, because of the asymmetric segregation of karmellae. During logarithmic phase growth, karmellae were the predominant membrane type, present in 50% of cells in the population. During early stationary phase, whorls became the predominant membrane type, present in nearly 50% of cells in the population. In later stationary phase growth, most membrane proliferations were lost so that few cells contained any observable membrane proliferations. However, in the small number of stationary phase cells that did possess membrane proliferations, only whorls were observed. Eventually, even these whorls disappeared from the cells.

At all stages except stationary phase, ~10–20% of cells contained more than one type of membrane or intermedi-

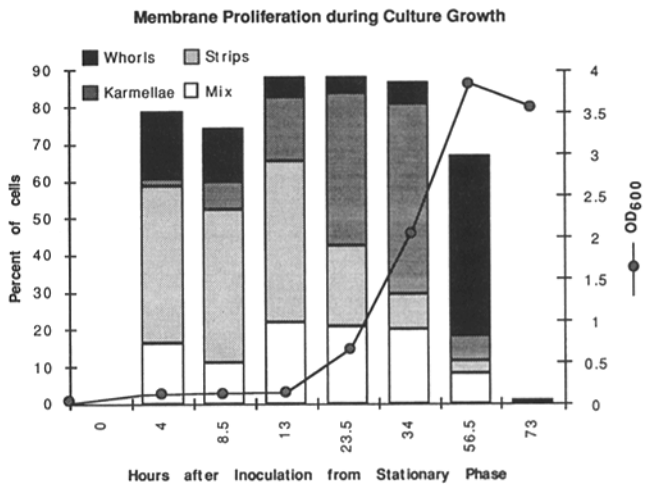

Figure 3. The types of membranes induced by Hmg1p were related to the growth phase of the culture and to the amount of Hmg1p. This graph represents the time course of membrane proliferations observed in populations expressing *HMG1* from the *adh+* promoter. Membrane organization was determined by observation of $DiOC_6$-stained cells. Data were pooled from two independent experiments with at least 100 cells assayed per each time point. Cells with multiple types of membranes or with intermediate membrane types are grouped together as "Mix."

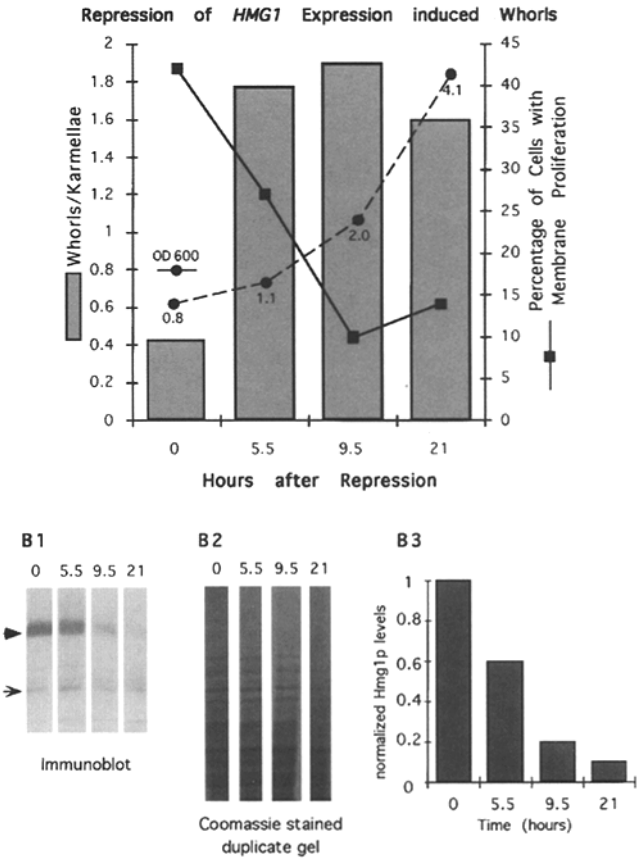

Figure 4. Repression of *HMG1* expression from the *nmt+* promoter induced loss of karmellae and formation of whorls which were subsequently degraded. (*A*) The bars on this graph show the increase in the ratio of cells with whorls versus karmellae following expression of *HMG1* from the *nmt1+* promoter was repressed by the addition of thiamine. At 9.5 and 21 h after repression, similar proportions of cells containing whorls were observed. However, the whorls in these cells were thinner than those present after 5.5 h, suggesting that the whorls were being degraded. As the proportion of cells with whorls relative to karmellae increased, the proportion of the cell with membrane proliferation decreased (line with square data points). The increase in OD_{600} is shown on the line with circular data points. (*B1*) Immunoblots using anti-Hmg1p antiserum from the time points in *4A* showed that the steady state levels of Hmg1p decreased following addition of thiamine. Serial dilutions (not shown) confirmed that the alkaline phosphatase reactions shown on this blot were in the linear range. (*B2*) Duplicate of the SDS polyacrylamide gel that was used for the immunoblot in B1 shown as a control for total protein loading. (*B3*) Both the immunoblot and the Coomassie stained duplicate gel were digitized and then analyzed using NIH Image Analysis software. The graph shows the levels of Hmg1p on the immunoblot, normalized to total protein. These calculations do not take into account the dilution of Hmg1p due to cell division. If the dilution factor is taken into account, a decreasing trend is also observed, indicating that the amount of Hmg1p per cell is still decreasing albeit less sharply. Arrowhead, Hmg1p (115 kD). Arrow, Hmg1p main breakdown product (~60 kD).

ate forms that were not readily scorable as a peripheral strip, karmellae, or whorls (for example see Fig. 11 *A*). The relationship between the peripheral strips formed during lag phase growth and other membrane types is currently under investigation and will not be discussed in this report, which focuses on the karmellae and whorl membranes.

To examine further the relationship between karmellae and whorls, we constructed pPL283, which placed *HMG1* under control of *nmt*+, a repressible *S. pombe* promoter. This promoter is active in the absence of thiamine, but is repressed by the presence of thiamine (21, 38). Expression of *HMG1* from the *nmt1*+ promoter was induced for 24 h by growth of cells containing pPL283 in the absence of thiamine, to allow karmellae to accumulate. Then, thiamine was added to repress *HMG1* expression. Using $DiOC_6$ staining, the membrane arrays in these cells were then observed for the next 21 h. Consistent with previous observations of cells expressing *HMG1* from the *adh*+ promoter, as the percentage of cells with karmellae decreased, a concomitant increase in the percentage of cells with whorls was observed. As the membranes were degraded, there was an increase in the number of cells with whorls relative to the number of cells with karmellae (Fig. 4 *A*). At the same time, there was a corresponding decrease in Hmg1p levels (Fig. 4 *B*) and the proportion of cells with proliferated membranes decreased from greater than 40% of cells in the population to ~10%. As a control, the whorl to karmellae ratios in a minus thiamine culture and a plus thiamine culture were also compared in a separate set of experiments (data not shown). Results showed that the whorl to karmellae ratio was higher when *HMG1* expression was repressed with thiamine compared to when *HMG1* expression was not repressed, reconfirming that the increase in whorl formation seen in Fig. 4 was due to the repression of the *HMG1* gene. Although the time-course of the expression of *HMG1* was different when expressed from the *adh*+ versus the *nmt1*+ promoter, observations using both promoters were consistent and supported the possibility that the whorls were intermediates in karmellae degradation.

The Cytoplasmic Whorls Enclosed Compartments That Were Distinct from Preexisting Vacuoles

Results from both ultrastructural and $DiOC_6$ staining suggested that whorls were formed from pockets of karmellae that pulled away from the nucleus and detached to form a multilayered membrane whorl that contained several vesicles or compartments (Figs. 1 and 2, see also Fig. 11). Electron micrographs showed that the interior of this compartment contained cytoplasm. Some aspects of the process of whorl formation appeared similar to autophagy, in which an ER-derived membrane cisterna curls around a portion of cytoplasm and fuses to sequester the engulfed cytoplasm in an autophagosome (17, 53, 58). Turnover of cytosolic components by autophagy requires conversion of the autophagosome into an acidic compartment, known as the autolysosome (17, 53). Thus, if whorls represented autophagic intermediates in karmellae degradation, we expected that their interior would become acidified and stain with CDCFDA, a fluorescent probe that has been used to study vacuoles in yeast (46, 48, 64, 65).

To test this possibility, we examined whorls in cells stained with CDCFDA. Consistent with our expectations, the interior of the whorl contained CDCFDA-stained vesicles. However, rather than being uniformly stained as expected for autophagosomes, the interior of the whorl con-

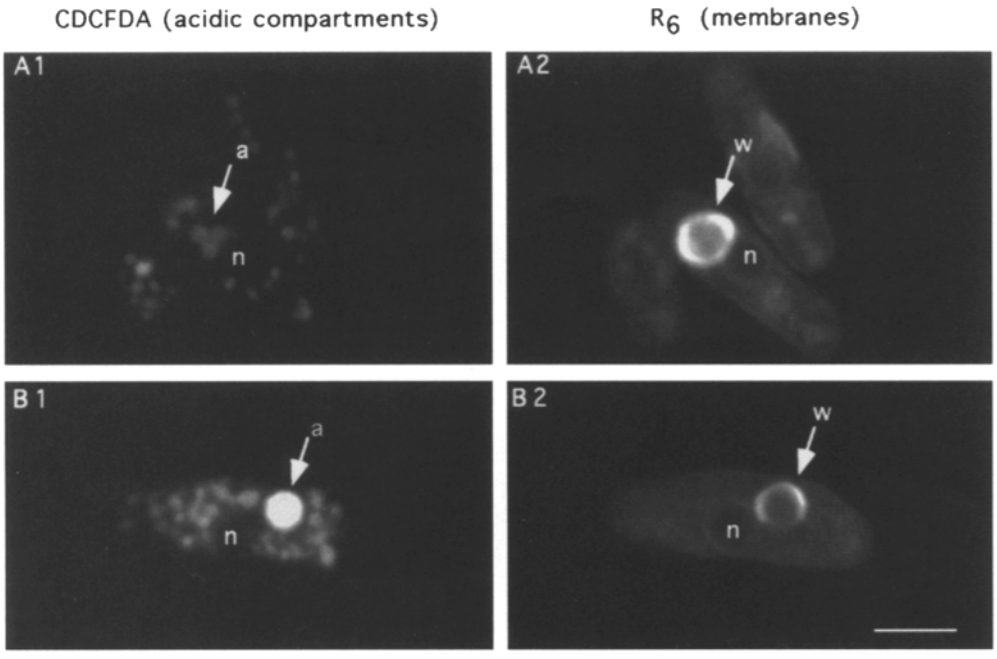

Figure 5. The interior of the whorl contained one or more compartments that stained with CDCFDA. Living cells expressing *HMG1* under control of the *nmt1*+ promoter were double-stained with CDCFDA to label vacuoles and with R6 to label the nuclear envelope, ER, and membrane proliferations. The left panels show CDCFDA staining and the right panels show R6 staining. (*A1* and *A2*) The membranes of the whorl were stained with R6 but did not stain with CDCFDA. Instead, CDCFDA stained three compartments in the interior of the whorl. (*B1* and *B2*) In rare cases, a whorl contained only one large CDCFDA-stained compartment, as shown in this figure. *a*, CDCFDA-stained compartment; *n*, nucleus; *w*, whorl. Bar, 5 μm.

tained one or more separate compartments (Fig. 5). To clarify further the structure of the whorl, serial thin sections were examined (data not shown). 12 out of 15 whorls examined were not completely closed but had one or more small openings to the surrounding cytoplasm. Nevertheless, all 15 whorls contained similar kinds of compartments, regardless of whether the structure was closed or open (see Fig. 2 for electron micrographs showing these compartments). These observations suggested that the whorl was unlike a typical autophagosome (7, 18).

To determine whether or not the CDCFDA-stained compartments in the whorl interior were preexisting vacuoles that were engulfed when the whorl detached from the nucleus, we took advantage of the *ade6* mutation present in our strains. Mutant yeast strains with defects in certain steps of adenine biosynthesis, including *ade6* strains, accumulate a fluorescent pigment in their vacuoles when the supply of adenine becomes limiting (65). Consequently, if the compartments in the whorl interior were engulfed vacuoles, the characteristic vacuole autofluorescence should be present in these compartments. Surprisingly, in greater than 95% of more than 300 whorls observed, the compartments present in the whorl interior did not contain the vacuolar *ade6* fluorochrome (Fig. 6). This result suggested that the compartments in the whorl might be different from vacuoles. However, the absence of the *ade6* fluorochrome could reflect the presence of whorl membranes, which prevented the engulfed vacuoles from accumulating the vacuole fluorochrome.

To test this possibility, karmellae were induced in cells grown in medium containing limiting amounts of adenine to allow accumulation of the red fluorochrome in all vacuoles before karmellae degradation. *HMG1* expression was then repressed by the addition of thiamine and karmellae were allowed to differentiate into whorls. Again, the whorls excluded preexisting vacuoles which had been marked by the accumulation of the red fluorochrome. This result ruled out the possibility that the absence of the fluorochrome from the compartments inside the whorls was merely due to the inability of the sequestered vacuoles to accumulate the red fluorochrome.

If the compartments in the whorls were distinct from preexisting vacuoles, two populations of CDCFDA-stained compartments should exist in cells undergoing karmellae degradation. There should be a population of stained compartments that lacked the *ade6* fluorochrome and another population of stained compartments that contained the *ade6* fluorochrome. Therefore, we examined the correlation between CDCFDA-stained compartments and vacuoles (stained with the *ade6* vacuole fluorochrome). In all cells that lacked karmellae, every compartment in a cell that was stained with CDCFDA also contained the vacu-

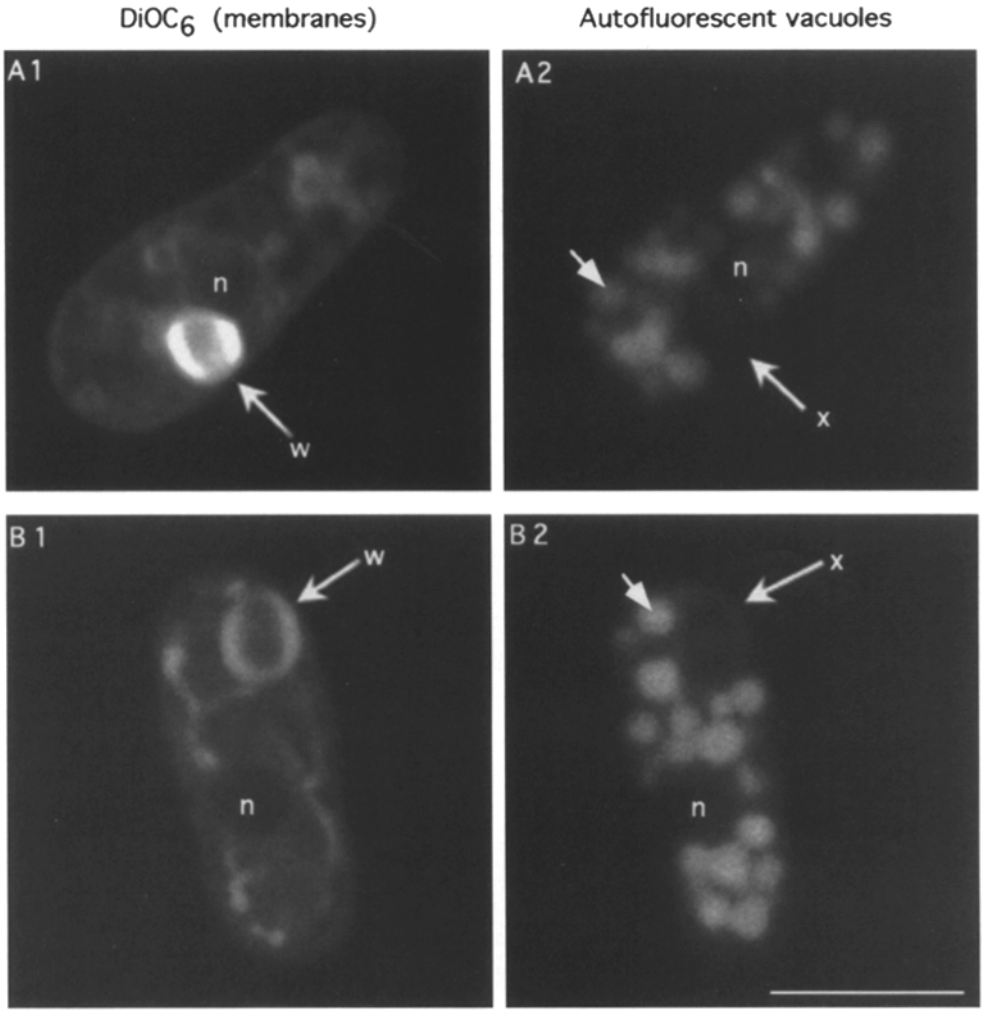

Figure 6. The interior of the whorl excluded preexisting vacuoles. Living cells expressing *HMG1* under control of the *nmt1+* promoter were stained with $DiOC_6$, which allowed visualization of the nuclear envelope, ER, and proliferated membranes (*left panels*). The right panels show vacuoles, stained with the endogenous fluorochrome that accumulates in the vacuoles of *ade6* cells. Vacuoles were excluded from the interior of more than 95% of whorls. Small arrow points to fluorochrome-containing vacuoles. Large arrows points to the whorl. *n*, nucleus; *w*, whorl; *x*, exclusion of the pigment containing vacuoles. Bar, 5 μm.

ole fluorochrome. However, in one-third of the cells in a population that was undergoing karmellae degradation, one to three CDCFDA-stained compartments were present per cell that did not contain the vacuole fluorochrome (Fig. 7). Interestingly, some of these fluorochrome-negative compartments were more intensely stained with CDCFDA than the fluorochrome-positive compartments. This result was consistent with the observation that compartments inside a whorl were often more intensely stained with CDCFDA than preexisting vacuoles (Fig. 5 *B*). In addition, the presence of one to three fluorochrome-negative compartments per cell was consistent with the presence of one or two whorls per cell. Thus, in cells that were degrading karmellae membranes, two populations of CDCFDA-stained compartments existed: preexisting vacuoles that contained the vacuole fluorochrome and newly formed compartments in the whorl that did not contain the vacuole fluorochrome (Fig. 7).

The Dye FM1-43, Which Labels Vacuolar Membranes, Did Not Stain Whorl Membranes or the CDCFDA-stained Compartments in the Whorl Interiors

To examine in greater detail the possibility that karmellae degradation involved a compartment that was distinct from preexisting vacuoles, we stained the vacuolar membranes in karmellae-containing cells with the fluorescent dye, FM1-43. This dye is trapped in the outer leaflet of the plasma membrane, and can be used to follow membranes of organelles in the endocytic pathway (57). To our knowledge FM1-43 has not been previously used in fungi, although a structurally similar dye, FM4-64, has been used to label yeast vacuoles (64). To show that FM1-43 stained the vacuolar membrane as expected, cells were double-stained with CDCFDA to stain the vacuole lumen and with FM1-43 (Fig. 8).

When wild-type *S. pombe* cells were grown in medium containing FM1-43, the outline of the cell was first observed, consistent with staining of the plasma membrane.

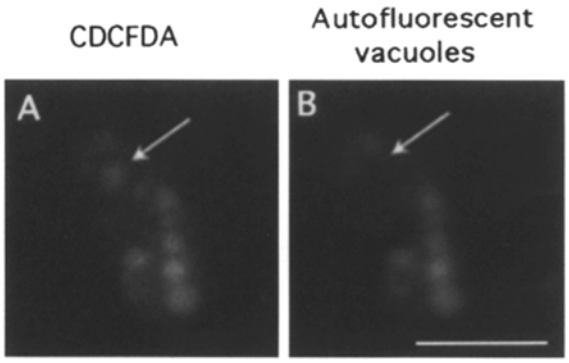

Figure 7. Two types of CDCFDA-stained compartments were present in cells with increased levels of Hmg1p. Living cells expressing *HMG1* under control of the *nmt1+* promoter were stained with CDCFDA. Then the pattern of CDCFDA staining was compared to the staining with the vacuole fluorochrome that accumulates in the vacuoles of *ade6* cells. One type of compartment contained the *ade6* fluorochrome and another type lacked the vacuole fluorochrome. Arrows point to a compartment stained with CDCFDA that lacked the *ade6* fluorochrome. Bar, 5 μm.

After 5 to 10 min, the cytoplasm of the cell was stained and bright patches were occasionally observed near the cell periphery. After 20 to 30 min, vacuolar membranes were stained (Fig. 8) This pattern of staining was consistent with the expectation that FM1-43 was entering the cells via an endocytic route, as demonstrated for FM4-64 (64). Karmellae were induced in the presence of FM1-43 and then allowed to undergo degradation. Thus, the vacuolar membranes were already labeled at the time of karmellae formation and continued to be labeled throughout induction and degradation. The FM1-43 staining pattern was then observed either in the absence or presence of $DiOC_6$, which allowed visualization of all ER membranes. In greater than 95% of the whorls, the enclosed vesicles were not labeled with FM1-43, further supporting the possibility that the compartments in whorl interiors were distinct from preexisting vacuoles (Fig. 9). In addition, neither karmellae membranes nor the whorls themselves were stained with FM1-43, indicating that there was no fusion between karmellae or whorl membranes with preexisting vacuoles or vesicles derived from endocytosis.

A Compartment Containing Neutral Lipids Accumulated in the Whorl Interior during Degradation

Under Nomarski optics, the whorls accumulated refractile spheres in the interior. These spheres appeared similar to lipid particles that are present in the cytoplasm of wild-type cells (51). However, the refractile spheres in the interior of the whorls grew larger as the whorls were degraded. Consequently, they were often larger than those observed in the cytoplasm of uninduced cells. We suspected that the refractile spheres represented the terminal morphological structure following karmellae degradation. If they were actually lipid particles, the refractile spheres should contain neutral lipid (32). To test for the presence of lipids in the refractile spheres, we stained cells with Nile Red, a fluorescent dye that stains neutral lipids, including sterol esters and neutral phospholipids (22). Nile Red is an uncharged benzophenoxasone dye composed of four conjugated rings and a hydrocarbon tail, resembling cholesterol. The fluorescent properties of Nile Red vary depending on the hydrophobic environment in which it is dissolved. When excited at wavelengths below 580 nm, Nile Red that is dissolved in lipid particles is preferentially observed and exhibits an intense, yellow-gold fluorescence. In contrast, excitation of the same cells at wavelengths greater than 580 nm reveal Nile Red fluorescence in cellular membranes that is less intense and red in color (22). In wild-type *S. pombe* cells, all refractile spheres were stained with Nile Red, indicating that these structures were indeed lipid particles. Exciting the dye at 488 nm allowed us to visualize the lipid particles simultaneously with cellular membranes. Thus, in contrast to $DiOC_6$ staining that labels only membranes, Nile Red stained both membranes and lipid particles, but each had a distinct intensity and color. When karmellae-containing cells were stained with Nile Red, karmellae membranes were readily observed. In addition, Nile Red also stained the refractile spheres that were enclosed within the whorl membranes. One or more such Nile Red-positive spheres were present within the whorl (Fig. 10). As degradation proceeded, the thickness

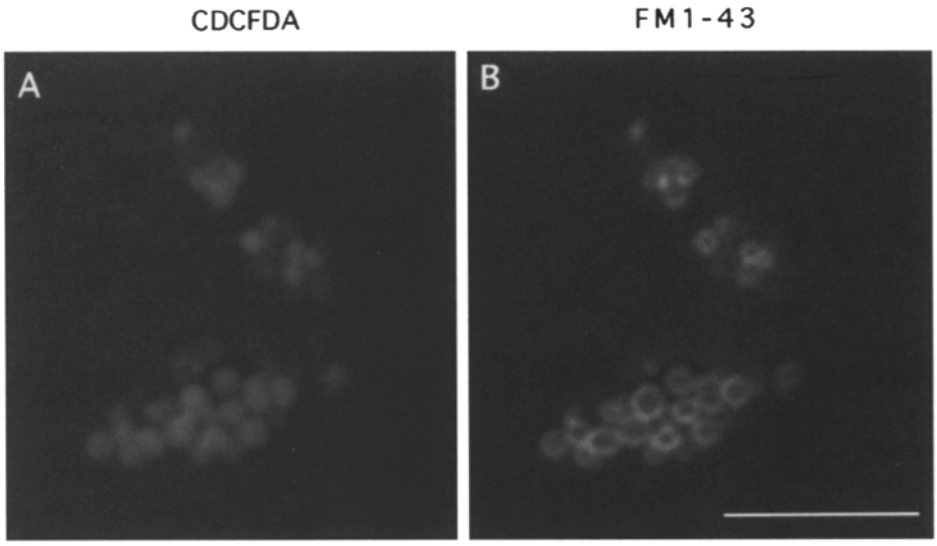

Figure 8. The lipophilic dye, FM1-43, labeled vacuole membranes in living cells. These cells, in which expression of *HMG1* was repressed by growth on thiamine-containing medium, were stained with FM1-43 to label vacuole membranes and with CDCFDA to label vacuole contents. *A* shows staining of vacuole interiors with CDCFDA. *B* shows FM1-43 staining of the vacuolar membranes. Bar, 5 μm.

of the whorl membranes decreased and the Nile Red-positive compartment grew larger. Thus, as karmellae membranes were degraded, it appeared that the resulting lipids were segregated into a lipid particle that formed in the whorl interior.

Cycloheximide Did Not Affect Formation of the Whorls or the Subsequent Accumulation of the Neutral Lipid Compartment

To gain further insight into the mechanics of karmellae degradation, we determined whether or not new protein synthesis was required for whorl formation. The synthesis of Hmg1p protein from the *nmt1*+ promoter was induced by growth of cells with pPL283 in thiamine-free medium to allow karmellae membranes to proliferate. After the cells reached the peak of karmellae production at mid-logarithmic phase of growth, expression of *HMG1* was repressed by addition of thiamine and 200 μg/ml of cycloheximide was added to stop protein synthesis (6, 45). Growth of the culture was arrested, showing that cycloheximide at this concentration was effective in preventing new protein synthesis (data not shown). Nevertheless, during the 4 h of observation, karmellae continued to detach from the nucleus to form cytoplasmic whorls. Furthermore, the interiors of the whorls developed the refractile lipid particles during the later stages of degradation (data not shown). Thus, the process of whorl formation (i.e., the detachment of karmellae from the nucleus) and at least the initial stages of lipid particle formation required no new protein synthesis. However, the whorl membranes were not completely degraded in the presence of cycloheximide, so that some lipid particles continued to be enclosed within whorl membranes.

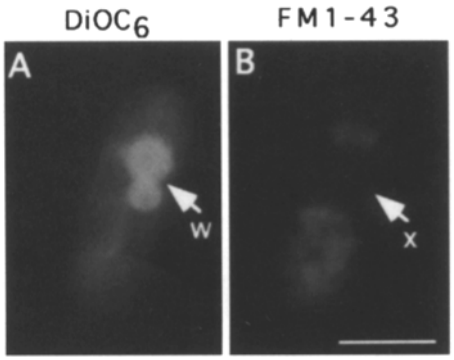

Figure 9. No organelle stained with FM1-43 was observed in the whorl interior. Living cells expressing *HMG1* under control of the *nmt1*+ promoter were grown in the presence of FM1-43 to label vacuolar membranes and then expression of *HMG1* was repressed by addition of thiamine to induce karmellae degradation. These cells were also stained with $DiOC_6$ to visualize whorl membranes. Vacuoles were generally excluded from the whorl interior (95% of observations). In addition, neither the whorls themselves nor the compartments within the whorl interior were labeled with FM1-43. *w*, whorl; *x*, exclusion of FM1-43 dye. Bar, 5 μm.

Interestingly, inhibition of new protein synthesis actually promoted the formation of whorls (Fig. 11 *A*). This result suggested that a short-lived protein may be needed for karmellae maintenance. The relative Hmg1p levels were essentially identical in cycloheximide-treated and in control cells during the experiment (Fig. 11, *B* and *C*). Thus, similar amounts of Hmg1p were present in cycloheximide-treated and control cells, even though the proportions of cells containing whorls or karmellae in these populations were significantly different. Populations of cycloheximide-treated cells had increased levels of whorls relative to karmellae relative to control cells. These data suggested that the presumptive short-lived protein needed for karmellae maintenance was not Hmg1p itself. Cycloheximide also had a similar effect on karmellae generated by constitutive expression of *HMG1* from the *adh*+ promoter (data not shown).

Discussion

A major pathway for turnover of cellular components, including organelles, is autophagy. During autophagy, portions of cytoplasm are sequestered into vesicles and delivered to the lysosome for degradation (18, 53, 54). Certain features of karmellae degradation appeared similar to autophagy. For example, the autophagosome membrane can

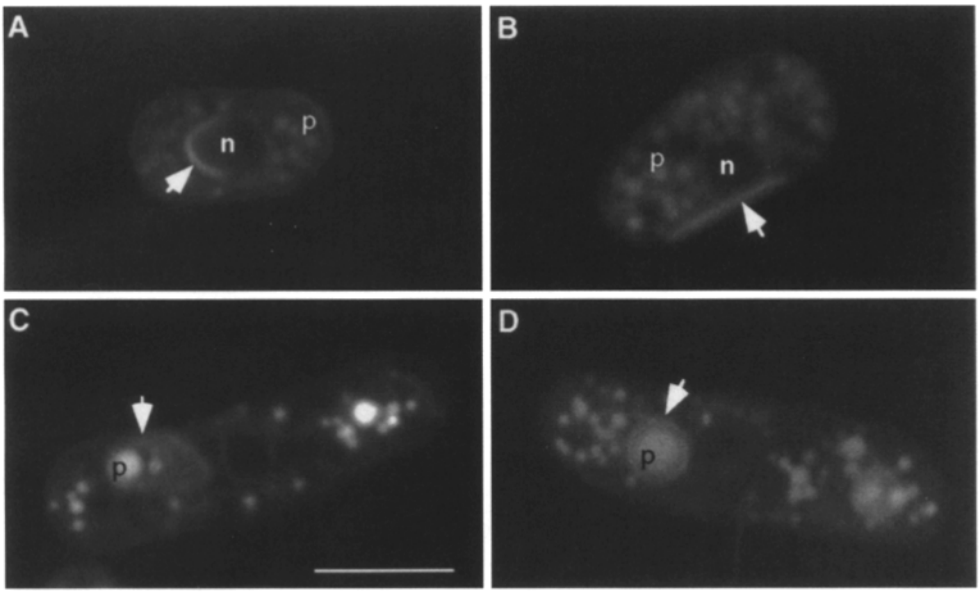

Figure 10. A neutral lipid compartment that stained with Nile Red was present in the whorl interior. Living cells expressing *HMG1* under control of the *nmt1*+ promoter were stained with Nile Red to visualize neutral lipid particles and membranes. (*A*) Karmellae membranes as well as lipid particles were stained with Nile Red. (*B*) Peripheral strips of stacked membranes, the nuclear envelope and lipid particles were stained with Nile Red. (*C* and *D*) Nile Red stained a lipid compartment in the interior of whorls. This compartment appeared highly refractile under Nomarski optics (not shown). As the whorl became thinner in the later stages of degradation, the lipid particle grew larger, so that a large lipid particle remained after the whorl was completely degraded. Arrows point to the proliferated membranes. *n*, nucleus; *p*, lipid particle. Bar, 5 μm.

be derived from ER membranes (18, 63) and can contain multiple membrane layers, similar to the whorls formed during karmellae degradation (for example, see references 9, 61, and 62). However, certain features of karmellae degradation distinguished it from autophagy. For example, the morphology of karmellae degradation differed from autophagy. Instead of forming a single compartment as in autophagy, small compartments formed within the whorl interior. The whorl was then degraded from the inside out, leaving a lipid particle. A further indication that karmellae degradation occurred by a non-autophagic process was the absence of a role for preexisting vacuoles in karmellae degradation. During autophagy, the autophagosome contents are delivered for digestion to a lysosome or prelysosomal compartment, or, in yeast, to the vacuole (7, 17, 18, 31, 53, 58). Our results demonstrated that karmellae degradation did not involve preexisting vacuoles. In addition, the lack of FM1-43 staining of whorl membranes indicated that these membranes did not fuse with vesicles derived from the endosomal pathway (see reference 64 for studies using a similar dye).

The lack of a role for preexisting vacuoles in karmellae degradation raises interesting questions concerning the source of the degradative enzymes for karmellae breakdown. New protein synthesis was required for only the terminal stages of karmellae degradation. Thus, at the time of formation, the whorls contained all of the proteins needed to at least partially degrade the membranes. The ability of karmellae to differentiate into a self-degradative organelle supports the possibility, raised by Noda and Farquhar, that a de novo mechanism may exist to convert ER-derived membranes into a degradative compartment (41). Their hypothesis was based on analysis of intracisternal granule degradation in thyrotrophs. These granules, which contain the beta-subunit of thyrotropic hormone, form within the ER lumen when secretion of thyrotropic hormone is induced, then abruptly repressed. The granules are too large to be cleared from the ER via the secretory pathway. Instead, the ER pinches off to enclose a granule in a vesicle delimited by a single membrane. The resulting compartment attains characteristics of lysosomes and the contents are degraded. Observations consistent with a de novo pathway for vacuole formation have also been obtained from studies of vacuole morphology mutants (47). The patterns of karmellae degradation indicated that ER-derived membranes in fission yeast could also differentiate into a degradative compartment. However, rather than simply digesting ER lumenal contents, the process of karmellae degradation resulted in degradation of the ER-derived membranes themselves.

Cycloheximide treatment prevents the mevalonate-accelerated turnover of HMG-CoA reductase in mammalian cells (12). However, our results showed that cycloheximide treatment did not prevent the initial step of karmellae degradation in *S. pombe* (see Fig. 11 *C*). Furthermore, instead of preventing formation of whorls, which were the morphological intermediate in karmellae degradation, inhibition of new protein synthesis induced rapid formation of whorls. This result suggested that a short-lived protein or proteins were needed for maintenance of karmellae. These proteins might be necessary to anchor karmellae to the outer nuclear envelope, thus preventing whorl formation. The short-lived protein needed for karmellae maintenance was not Hmg1p, since no difference in Hmg1p levels was found in cycloheximide-treated populations that had low numbers of karmellae-containing cells, and control

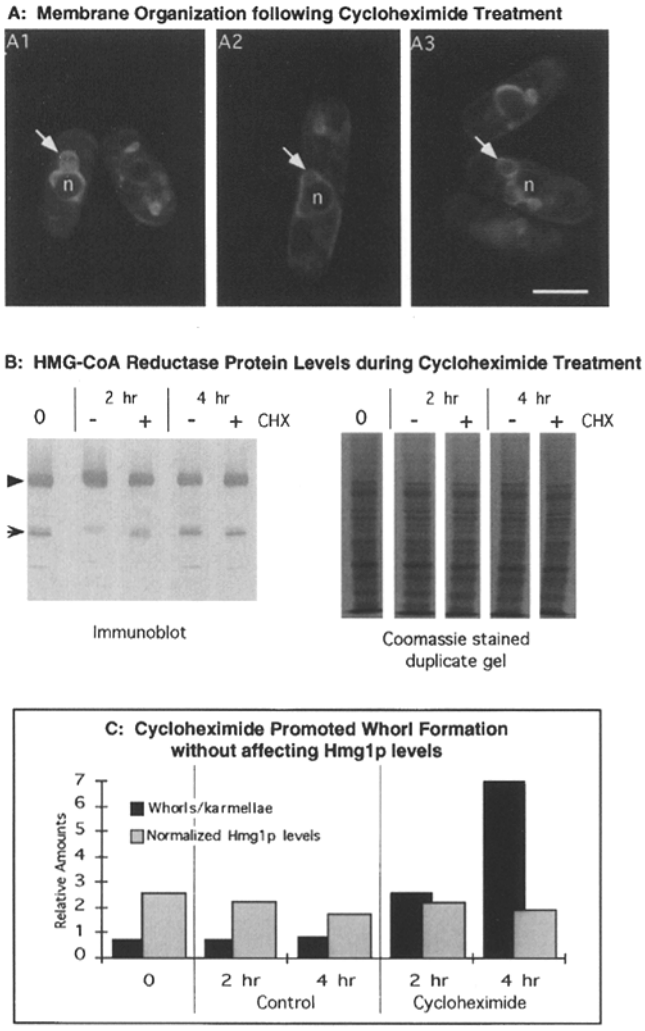

Figure 11. Inhibition of protein synthesis by cycloheximide did not inhibit whorl formation, but, instead, accelerated the process. Living cells expressing *HMG1* under control of the *nmt1*+ promoter were allowed to accumulate karmellae. At the peak of karmellae production, cycloheximide was added to inhibit protein synthesis and thiamine was added to repress transcription of *HMG1*. (*A*) Karmellae detached from the nucleus to form whorls in the presence of cycloheximide. Arrows show incipient whorls or whorls that have already detached from the nucleus. (*B*) Immunoblots using anti-Hmg1p antiserum showed that cells treated with cycloheximide had similar amounts of Hmg1p as controls. Serial dilutions (not shown) confirmed that the alkaline phosphatase reactions shown on this blot were in the linear range. Duplicate of the SDS–polyacrylamide gel that was used for the immunoblot is shown as a control for total protein loading. (*C*) Filled bars show the proportion of cells with whorls relative to karmellae following cycloheximide treatments. Gray bars show Hmg1p levels normalized to total protein. The whorls/karmellae ratio increased in the presence of cycloheximide, but no appreciable difference was observed in Hmg1p levels in the control and the cycloheximide treated cells. Arrowhead, Hmg1p (115 kD). Arrow, Hmg1p breakdown product (~60 kD). *n*, nucleus; CHX, cycloheximide 200 μg/ml.

populations that had high numbers of karmellae-containing cells. Thus, at least one protein other than HMG-CoA reductase must be involved in the formation or maintenance of karmellae. An alternate interpretation of these results is that, rather than requiring synthesis or presence of a specific protein, karmellae maintenance depends on a certain level of ongoing translation. We have isolated mutants that produce decreased amounts of karmellae and/or increased numbers of whorls (Chang, H., P. Y. Lum, and R. Wright, unpublished observations). Analysis of these mutants should shed light on these alternatives.

During the degradation process, both lipid particles and CDCFDA-stained compartments were present in the interior of whorls. However, the relationship between these two compartments remains unclear. Lipid particles in yeast have similar structures as mammalian lipoproteins, consisting of a neutral lipid core that contains steryl esters and triacylglycerols, and a monolayer containing both phospholipids and sterols (32). Our working hypothesis, based partially on models of apolipoprotein production (14) (Fig. 12), is that acidification of regions in the innermost whorl layer activates endogenous phospholipases, es-

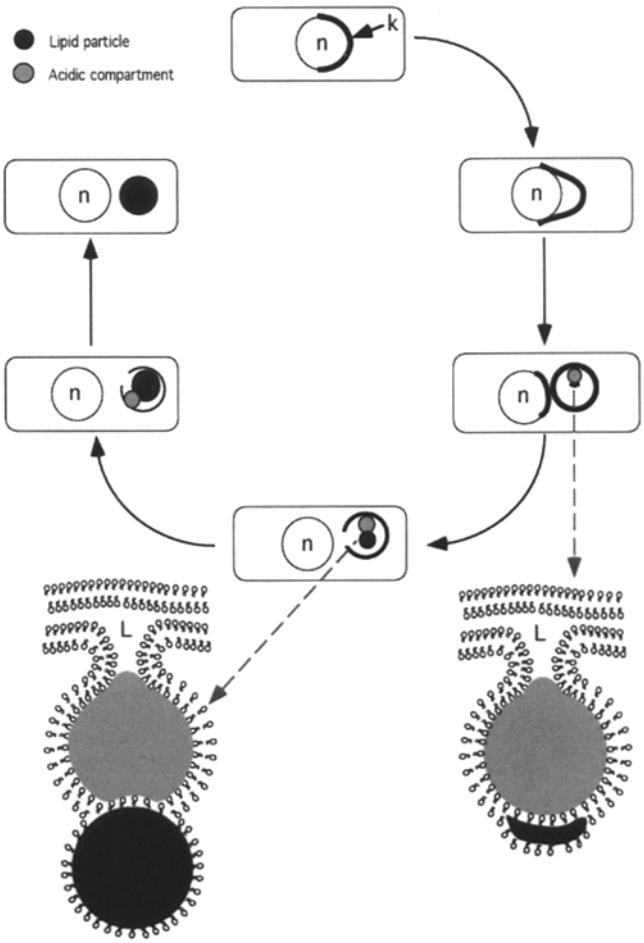

Figure 12. Working hypothesis of the mechanics of karmellae degradation. Karmellae detach from the nucleus to form a whorl of stacked membranes. This alteration activates proteins in the innermost layers of the whorl, causing portions of the membrane to dilate and the lumen of this dilated region to become acidic. The change in pH activates proteases, lipases, and esterases which degrade the membrane sequentially from the interior outward. Products of lipid degradation accumulate between the leaflets of the membrane, forming a lipid particle. The degradation continues until the whorl membranes have been completely degraded and only the lipid particle remains.

terases, and proteases. As these enzymes degrade the membrane proteins and lipids of the whorl, hydrophilic products accumulate in the acidic region and hydrophobic products accumulate between the monolayers, forming a lipid particle. After membrane degradation is complete, the lipid particle remains as a neutral lipid store, from which sterols and lipids may be obtained for membrane biogenesis (34, 59). The fate of the CDCFDA-stained compartments produced during karmellae degradation is currently unknown. One possibility is that these compartments fuse with or differentiate into vacuoles. Alternately, the contents of these compartments may be released into the cytoplasm, so that the compartment progressively disappears as membrane degradation is completed.

Karmellae degradation appeared morphologically similar to degradation of other ER membranes, including membranes induced in mammalian cells by phenobarbital (9) or HMG-CoA reductase (4). Ultrastructural analysis of crystalloid ER degradation shows that, concomitant with addition of LDL, the precise organization of crystalloid ER structure disintegrates (42). The crystalloid ER tubules dilate and the membranes are apparently degraded in situ, without any accumulation of autophagic structures. Electron micrographs of cells undergoing crystalloid ER degradation show formation of lipid particles near the disorganized crystalloid Er arrays, similar to those seen in the whorl interior (Fig. 10 *C* in reference 4). Although the morphological details of karmellae and crystalloid ER degradation differ, degradation of both membrane arrays appears to occur by conversion of the ER-derived membranes into self-degradative compartments. Thus, the mechanisms by which HMG-CoA reductase induced membranes are degraded may be conserved.

Our results suggested that, in fission yeast, the degradation of Hmg1p and karmellae membranes may be coupled. In mammalian cells, HMG-CoA reductase turnover is thought to be coordinated with, but independent of crystalloid ER degradation. This conclusion is based on the observation that decreases in the amount of HMG-CoA reductase activity preceded degradation of crystalloid ER (4, 42). In these studies, crystalloid ER turnover was measured by loss of the total volume occupied by crystalloid ER elements. However examination of the published micrographs shows that the surface area of the crystalloid ER decreased before decreases in the total volume were observed and that the decrease in surface area was correlated with the decrease in HMG-CoA reductase activity. Specifically, 8 h after addition of LDL, HMG-CoA reductase activity decreased 1.76-fold (Table 3 in reference 42). Our morphometric analysis of Figs. 2 *A* and 10 *A* (in reference 4) shows that the surface area of crystalloid ER tubules also had decreased ~1.8-fold. Thus, in mammalian cells, degradation of HMG-CoA reductase may also occur simultaneously with loss of the membranes in which the protein is localized. However, to what degree the degradation of the protein and the membranes is coupled in the fission yeast is a question for future investigation.

Many proteins, including unfolded or mutant secretory proteins and ER-resident proteins, are degraded within the ER in a process that does not involve lysosomes and is characterized by the lack of Golgi-type glycosylation of the substrates (10, 20, 35). Degradation of HMG-CoA reductase itself has these characteristics and is signaled by increased cholesterol accumulation in the ER membrane (12, 24, 42). However, the correlation between the degradation of the ER proteins and the membranes in which they reside has not been determined in any cell type. If the degradation of HMG-CoA reductase-induced membranes represents a magnified view of normal ER turnover, then further studies on the relationship between the degradation of HMG-CoA reductase protein and HMG-CoA reductase-induced membranes should help clarify this issue.

We thank M. Terasaki for suggesting the use of FM1-43, A. Alberts for the gift of lovastatin, and L. Goetsch and B. Byers for use of their transmission electron microscope. P. Brunner gave invaluable advice on confocal microscopy and image analysis. We thank C. Roberts and other members of our lab for critical reading of the manuscript and for suggestions and lively discussions.

This work was supported by National Institutes of Health Grant GM45726.

Received for publication 13 April 1995 and in revised form 15 June 1995.

References

1. Alberts, A. W., J. Chen, G. Kuron, V. Hunt, J. Huff, C. Hoffman, J. Rothrock, M. Lopez, H. Joshua, E. Harris et al. 1980. Mevinolin: a highly potent competitive inhibitor of hydroxymethylglutarly-coenzyme A reductase and a cholesterol-lowering agent. *Proc. Natl. Acad. Sci. USA.* 77: 3957–3961.
2. Alfa, C., P. Fantes, J. Hyams, M. McLeod, and E. Warbrick. 1992. Experiments with Fission Yeast. Cold Spring Harbor Laboratory Press, Cold Spring Harbor, NY. 169 pp.
3. Anderson, R. E., D. J. Landis, and P. A. Dudley. 1976. Essential fatty acid deficiency and renewal of rod outer segments in the albino rat. *Invest. Opthalmol.* 15:232–236.
4. Anderson, R. G. W., L. Orci, M. S. Brown, L. M. Segura, and J. L. Goldstein. 1983. Ultrastructural analysis of crystalloid endoplasmic reticulum in UT-1 cells and its disappearance in response to cholesterol. *J. Cell Sci.* 63:1–20.
5. Ausubel, F. M., R. Brent, R. E. Kingston, D. D. Moore, J. G. Seidman, J. A. Smith, K. Struhl, L. M. Albright, D. M. Moen, and A. Varki. 1994. Current Protocols in Molecular Biology. K. Janssen, editor. John Wiley & Sons, NY.
6. Ayscough, K., and G. Warren. 1994. Inhibition of protein synthesis disrupts the golgi apparatus in the fission yeast, *Schizosaccharomyces pombe. Yeast.* 10:1–11.
7. Baba, M., K. Takeshige, N. Baba, and Y. Ohsumi. 1994. Ultrastructural analysis of the autophagic process in yeast: detection of autophagosomes and their characterization. *J. Cell Biol.* 124:903–913.
8. Basson, M. E., M. K. Thorsness, J. Finer-Moore, R. Stroud, and J. Rine. 1988. Structural and functional conservation between yeast and human 3-hydroxy-3-methylglutaryl coenzyme A reductases, the rate-limiting enzyme of sterol biosynthesis. *Mol. Cell. Biol.* 9:3797–3808.
9. Bolender, R. P., and E. R. Weibel. 1973. A morphometric study of the removal of phenobarbital-induced membranes from hepatocytes after cessation of treatment. *J. Cell Biol.* 56:746–761.
10. Bonifacino, J. S., and J. Lippincott-Schwartz. 1991. Degradation of proteins within the endoplasmic reticulum. *Curr. Opin. Cell Biol.* 3:592–600.
11. Chin, D. J., K. L. Luskey, R. G. W. Anderson, J. R. Faust, J. L. Goldstein, and M. S. Brown. 1982. Appearance of crystalloid endoplasmic reticulum in compactin-resistant Chinese hamster cells with a 500-fold elevation in 3-hydroxy-3-methylglutaryl coenzyme A reductase. *Proc. Natl. Acad. Sci. USA.* 79:1185–1189.
12. Chun, K. T., S. Bar-Nun, and R. D. Simoni. 1990. The regulated degradation of 3-hydroxy-3-methylglutaryl-CoA reductase requires a short-lived protein and occurs in the endoplasmic reticulum. *J. Biol. Chem.* 265: 22004–22010.
13. Dallner, G., and J. W. DePierre. 1983. Membrane induction by drugs. *Method Enzymol.* 96:542–557.
14. Davis R. A. 1993. The endoplasmic reticulum is the site of lipoprotein assembly and regulation of secretion. *In* Subcellular Biochemistry. Vol. 21. N. Boorgese and J. R. Harris, editors. Plenum Press, NY. 169–187.
15. Deschenes, R. J., and J. R. Broach. 1987. Fatty acylation is important but not essential for *Saccharomyces cerevisiae RAS* function. *Mol. Cell. Biol.* 7:2344–2351.
16. deVries, E., J. P. vanderWeij, C. J. P. vanderVeen, and A. Cats. 1983. Characterization and classification of lymphoid cells after pokeweed mitogen stimulation. *Virchows Arch. Cell. Pathol.* 43:17–30.
17. Dunn, W. A. 1994. Autophagy and related mechanisms of lysosome-medi-

ated protein degradation. *Trends Cell Biol.* 4:139–143.
18. Dunn, W. A. J. 1990. Studies on the mechanisms of autophagy: Formation of the autophagic vacuole. *J. Cell Biol.* 110:1923–1933.
19. Endo, A., M. Kuroda, and K. Tanzawa. 1976. Competitive inhibition of 3-hydroxy-3-methylglutaryl coenzyme A reductase by ML-236A and ML236B fungal metabolites, having hypocholesterolemic activity. *FEBS Lett.* 72:323–326.
20. Finger, A., M. Knop, and D. H. Wolf. 1993. Analysis of two mutated vacuolar proteins reveals a degradation pathway in the endoplasmic reticulum or a related compartment of yeast. *Eur. J. Biochem.* 218:565–574.
21. Forsburg, S. L. 1993. Comparison of *Schizosaccharomyces pombe* expression systems. *Nucleic Acids Res.* 21:2955–2956.
22. Greenspan, P., and S. D. Fowler. 1985. Biological applications of the fluorescent lipid probe, Nile Red. *Kodak Laboratory Chemicals Bulletin.* 56: 1–6.
23. Greenspan, P., E. P. Mayer, and S. D. Fowler. 1985. Nile Red: a selective fluorescent stain for intracellular lipid droplets. *J. Cell Biol.* 100:965–973.
24. Hampton, R. Y., and J. Rine. 1994. Regulated degradation of HMG-CoA reductase, an integral membrane protein of the endoplasmic reticulum, in yeast. *J. Cell Biol.* 125:299–312.
25. Hancock, K., and V. C. W. Tsang. 1983. India ink staining of proteins on nitrocellulose paper. *Anal. Biochem.* 133:157–162.
26. Harlow, E., and D. Lane. 1988. Antibodies, A Laboratory Manual. Cold Spring Harbor Press, Cold Spring Harbor, NY. 726 pp.
27. Jack, E. M., W. Staubli, F. Waechter, P. Bentley, J. Suter, F. Bieri S. F. Muakkassah-Kelly, and L. M. Cruz-Orive. 1990. Ultrastructural changes in chemically induced preneoplastic focal lesions in the rat liver: a sterological study. *Carcinogenesis.* 11:1531–1538.
28. Jones, A. L., and D. W. Fawcett. 1966. Hypertrophy of the agranular endoplasmic reticulum in hamster liver induced by phenobarbital (with a review of the functions of this organelle in liver). *J. Histochem. Cytochem.* 14:215–231.
29. Koning, A. J., P. Y. Lum, J. M. Williams, and R. Wright. 1993. $DiOC_6$ staining reveals organelle structure and dynamics in living yeast cells. *Cell Motil. Cytoskel.* 25:111–128.
30. Laemmli, E. K. 1970. Cleavage of structural proteins during the assembly of the head of bacteriophage T4. *Nature (Lond.).* 227:680–685.
31. Lawrence, B. P., and W. J. Brown. 1992. Autophagic vacuoles rapidly fuse with pre-existing lysosomes in cultured hepatocytes. *J.Cell Sci.* 102:515–526.
32. Leber, R., E. Zinser, G. Zellnig, F. Paltauf and G. Daum. 1994. Characterization of lipid particles of the yeast, *Saccharomyces cerevisiae. Yeast.* 10: 1421–1428.
33. Lentz, T. L. 1971. Cell Fine Structure: An Atlas of Drawings of Whole-Cell Structure. W. B. Saunders, Philadelphia. 437 pp.
34. Lewis, T. A., R. J. Rodriguez, and L. W. Parks. 1987. Relationship between intracellular sterol content and sterol esterification and hydrolysis in *Saccharomyces cerevisiae. Biochem. Biophys. Acta.* 921:205–212.
35. Lippincott-Schwartz, J., J. S. Bonifacino, L. C. Yuan, and R. D. Klausner. 1988. Degradation from the endoplasmic reticulum: disposing of newly synthesized proteins. *Cell.* 54:209–220.
36. Maniatis, T., E. F. Fritsch, and J. Sambrook. 1982. Molecular Cloning, A Laboratory Manual. Cold Spring Harbor Press, Cold Spring Harbor, NY. 545 pp.
37. Matsumoto, B., D. M. Defoe, and J. C. Besharse. 1987. Membrane turnover in rod photoreceptors: ensheathment and phagocytosis of outer segment distal tips by pseudopodia of the retinal pigment epithelium. *Proc. R. Soc. London B. Biol. Sci.* 230:339–354.
38. Maundrell, K. 1990. *nmt1* of fission yeast. *J. Biol. Chem.* 265:10857–10864.
39. McLeod, M., and D. H. Beach. 1987. Homology between the *ran1+* gene of the fission yeast and protein kinases. *EMBO J.* 5:3665–3671.
40. Moreno, S., A. Klar, and P. Nurse. 1991. Molecular biology of the fission yeast *Schizosaccharomyces pombe. In* Guide to Yeast Genetics and Molecular Biology. Vol 194. C. Guthrie and G. Fink, editors. Academic Press, San Diego. 795–823.
41. Noda, T., and M. G. Farquhar. 1992. A non-autophagic pathway for diversion of ER secretory proteins to lysosomes. *J. Cell Biol.* 119:85–97.
42. Orci, L., M. S. Brown, J. L. Goldstein, L. M. Garcia-Segura, and R. G. W. Anderson. 1984. Increase in membrane cholesterol: a possible trigger for degradation of HMG-CoA reductase and crystalloid endoplasmic reticulum. *Cell.* 36:835–845.
43. Orrenius, S., and J. L. E. Ericsson. 1966. Enzyme-membrane relationship in phenobarbital induction of synthesis of drug-metabolizing enzyme system and proliferation of endoplasmic membranes. *J. Cell Biol.* 28:181–198.
44. Pathak, R. K., K. L. Luskey, and R. G. W. Anderson. 1986. Biogenesis of the crystalloid endoplasmic reticulum in UT-1 cells: evidence that newly formed endoplasmic reticulum emerges from the nuclear envelope. *J. Cell Biol.* 102:2158–2168.
45. Polanshek, M. M. 1977. Effects of heat shock and cycloheximide on growth and division of the fission yeast, *Schizosaccharomyces pombe. J. Cell Sci.* 23:1–23.
46. Pringle, J. R., R. A. Preston, A. E. M. Adams, T. Stearns, D. G. Drubin, B. K. Haarer, and E. W. Jones. 1989. Fluorescence microscopy methods for yeast. *Methods Cell Biol.* 31:357–435.
47. Raymond, C. K., I. Howald-Stevenson, C. A. Vater, and T. H. Stevens. 1992. Morphological classification of the yeast vacuolar protein sorting mutants: evidence for a prevacuolar compartment in class E vps mutants. *Mol. Biol. Cell.* 3:1389–1402.
48. Raymond, C. K., P. J. O'Hara, G. Eichinger, J. H. Rothman, and T. H. Stevens. 1990. Molecular analysis of the yeast VPS3 gene and the role of its product in vacuolar protein sorting and vacuolar segregation during the cell cycle. *J. Cell Biol.* 111:877–892.
49. Reynolds, E. S. 1963. The use of lead citrate at high pH as an electron-opaque stain in electron microscopy. *J. Cell Biol.* 17:208–212.
50. Rine, J., W. Hansen, E. Hardeman, and R. W. Davis. 1983. Targeted selection of recombinant clones through gene dosage effects. *Proc. Natl. Acad. Sci. USA.* 80:6750–6754.
51. Robinow, C. F., and J. S. Hyams. 1989. General cytology of fission yeasts. *In* Molecular Biology of the Fission Yeast. A. Nasim, P. Young, and B. F. Johnson, editors. Academic Press, San Diego. 273–330.
52. Russell, P. R., and B. D. Hall. 1983. The primary structure of the alcohol dehydrogenase gene from the fission yeast *Schizosaccharomyces pombe. J. Biol. Chem.* 258:143–149.
53. Seglen, P. O., and P. Bohley. 1992. Autophagy and other vacuolar protein degradation mechanisms. *Experientia.* 48:158–172.
54. Seglen, P. O., P. B. Gordon, and I. Holen. 1990. Non-selective autophagy. *Semin. Cell Biol.* 1:441–448.
55. Shapiro, D. J., and V. W. Rodwell. 1971. Regulation of hepatic 3-hydroxy-3-methylglutaryl coenzyme A reductase and cholesterol synthesis. *J. Biol. Chem.* 246:3210–3216.
56. Shohat, M., G. Janossy, and R. R. Dourmashkin. 1973. Development of rough endoplasmic reticulum in mouse splenic lymphocytes stimulated by mitogens. *Eur. J. Immunol.* 3:680–687.
57. Stafford, S. J., S. L. Shorte, and J. G. Schofield. 1993. Use of a fluorescent dye to measure secretion from intact bovine anterior pituitary cells. *Bio-Sci. Rep.* 13:9–17.
58. Takeshige, K., M. Baba, S. Tsuboi, T. Noda, and Y. Ohsumi. 1992. Autophagy in yeast demonstrated with proteinase-deficient mutants and conditions for its induction. *J. Cell Biol.* 119:301–311.
59. Taylor, F. R., and L. W. Parks. 1978. Metabolic interconversion of free sterols and steryl esters in Saccharomyces cerevisiae. *J. Bacteriol.* 136:531-537.
60. Terasaki, M. 1989. Fluorescent labeling of endoplasmic reticulum. *Methods Cell Biol.* 29:125–135.
61. Terasaki, M., J. Song, J. R. Wong, M. J. Weiss, and L. B. Chen. 1984. Localization of endoplasmic reticulum in living and glutaraldehyde-fixed cells with fluorescent dyes. *Cell.* 38:101–108.
62. Tuttle, D. L., A. S. Lewin, and J. W. A. Dunn. 1993. Selective autophagy of peroxisomes in methylotrophic yeasts. *Eur. J. Cell Biol.* 60:283–290.
63. Ueno, T., D. Muno, and E. Kominami. 1991. Membrane markers of endoplasmic reticulum preserved in autophagic vacuolar membranes isolated from leupeptin-administered rat liver. *J. Biol. Chem.* 266:18995–18999.
64. Vida, T. A., and S. D. Emr. 1995. A new vital stain for visualizing vacuolar membrane dynamics and endocytosis in yeast. *J. Cell Biol.* 128:779–792.
65. Weisman, L. S., R. Bacallao, and W. Wickner. 1987. Multiple methods of visualizing the yeast vacuole permit evaluation of it morphology and inheritance during the cell cycle. *J. Cell Biol.* 105:1539–1547.
66. Weist, D. L., J. K. Burkhardt, S. Hester, M. Hortsch, D. I. Meyer, and Y. Argon. 1990. Membrane biogenesis during B cell differentiation: most endoplasmic reticulum proteins are expressed coordinately. *J. Cell Biol.* 110:1501–1511.
67. Wright R. 1993. Insights from Inducible Membranes. *Curr. Biol.* 3:870–873.
68. Wright, R., M. Basson, L. D'Ari, and J. Rine. 1988. Increased amounts of HMG-CoA reductase induce "karmellae": a proliferation of stacked membrane pairs surrounding the yeast nucleus. *J. Cell Biol.* 107:101–114.
69. Wright, R., G. Keller, S. J. Gould, S. Subramani, and J. Rine. 1990. Cell-type control of membrane biogenesis induced by HMG-CoA reductase overproduction. *New Biologist.* 2:915–921.
70. Wright, R., and J. Rine. 1989. Transmission electron microscopy and immunocytochemical studies of yeast: analysis of HMG-CoA reductase overproduction by electron microscopy. *Methods Cell Biol.* 31:473–512.
71. Young, R. W. 1967. The renewal of photoreceptor outer segments. *J. Cell Biol.* 33:61–72.
72. Zucker-Franklin, D., M. F. Greaves, C. E. Grossi, and A. M. Marmont. 1988. Atlas of Blood Cells: Function and Pathology. Vol. 2. edi. Ermes, Milano. 653 pp.